

FILE COPY
ESD-TR-75-165

ESD ACCESSION LIST

XFRRI Call No. 82611

Copy No. 1 of 2 cys.

Technical Note

1975-21

M. L. Burrows

Losses in a Periodically Gapped Cable Armor in Contact with the Surrounding Soil

25 April 1975

Prepared for the Department of the Navy
under Electronic Systems Division Contract F19628-73-C-0002 by

Lincoln Laboratory

MASSACHUSETTS INSTITUTE OF TECHNOLOGY

LEXINGTON, MASSACHUSETTS



Approved for public release; distribution unlimited.

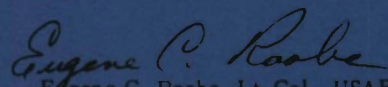
ADA010592

The work reported in this document was performed at Lincoln Laboratory,
a center for research operated by Massachusetts Institute of Technology.
The work was sponsored by the Department of the Navy under Air Force
Contract F19628-73-C-0002.

This report may be reproduced to satisfy needs of U.S. Government agencies.

This technical report has been reviewed and is approved for publication.

FOR THE COMMANDER



Eugene C. Raabe
Eugene C. Raabe, Lt. Col., USAF
Chief, ESD Lincoln Laboratory Project Office

MASSACHUSETTS INSTITUTE OF TECHNOLOGY
LINCOLN LABORATORY

LOSSES IN A PERIODICALLY GAPPED CABLE ARMOR
IN CONTACT WITH THE SURROUNDING SOIL

M. L. BURROWS
Group 61

TECHNICAL NOTE 1975-21

25 APRIL 1975

Approved for public release; distribution unlimited.

LEXINGTON

MASSACHUSETTS

ABSTRACT

A variational method is presented for evaluating the effective impedance of the periodically-gapped armor on a buried cable. The armor is assumed to be in direct contact with the surrounding soil, so that the gaps, which are intended to break the longitudinal electrical conductivity, are in fact electrically bridged by the soil. From the effective impedance can be calculated the armor losses and, when the cable is used as a buried antenna, the reduction in antenna efficiency.

Numerical results are presented graphically, and some corroborating experimental evidence is reported.

Losses in a Periodically Gapped Cable Armor
in Contact with the Surrounding Soil

I. Introduction

To prevent damage by rodents and insects to a directly buried cable, it is the practice to encase it in a metallic tape armor [1,2]. However, if the cable has a single conductor, the current induced in this conducting armor can dissipate an appreciable quantity of power [3] and when the cable is used as a buried antenna, the armor current also reduces the current moment of the antenna [4].

These detrimental effects can be reduced by breaking the electrical continuity of the armor at regular intervals to raise its effective longitudinal impedance. This raises the design problem of deciding how far apart the gaps can be placed without their current limiting function being negated by the electrical bridging effect of the surrounding soil.

In the following sections a variational method is proposed for evaluating the effective longitudinal impedance of a periodically-gapped armor in contact with the surrounding soil. This quantity is equal to the resistance per unit length of the armor, when the armor is continuous, and is used in its stead, for calculating the electrical effects of interest, when the armor is periodically gapped.

It is assumed throughout that the monochromatic time behavior is as $\exp(j\omega t)$ and that in the soil the quasi-static approximation $\omega\epsilon/\sigma = 0$ is valid, where ω is the radian frequency and ϵ and σ are the permittivity and conductivity of the soil.

II. The Armor Impedance

The cable-armor combination is modelled as an infinitely long circular dielectric cylinder of radius a at the surface of which is placed a sequence of resistive cylindrical sheets, each of length $2l - 2w$ and separated by gaps of width $2w$, (Fig. 1). The exterior medium is characterized by the conductivity σ and permeability μ .

At the low frequencies of interest here, the skin depth of conventional armor materials is sufficiently large compared with the armor thickness that the armor can be regarded as essentially resistive. Thus the resistive cylindrical sheets in the model have a resistance R_x , in ohm/meter, given by

$$R_s = \frac{\rho}{2\pi a \tau} \quad (1)$$

where ρ is the bulk resistivity and τ the thickness of the armor material.

The total z-directed electric field at the cylinder surface is the sum of the uniform "incident" field E_i , whose source remains at present unspecified, and the non-uniform "scattered" field $E_s(z)$ due to the current $I(z)$ induced in the armor. Over that part of the surface occupied by the resistive sheets, this field is equal to $I(z)R_s$. Thus, by taking advantage of the periodicity of the problem an integral equation for $I(z)$ can be written as

$$\begin{aligned} I(z)R_s + E_g(z) &= E_i + E_s(z) \\ &= E_i + \int_0^l G(z, z') I(z') dz', \end{aligned} \quad (2)$$

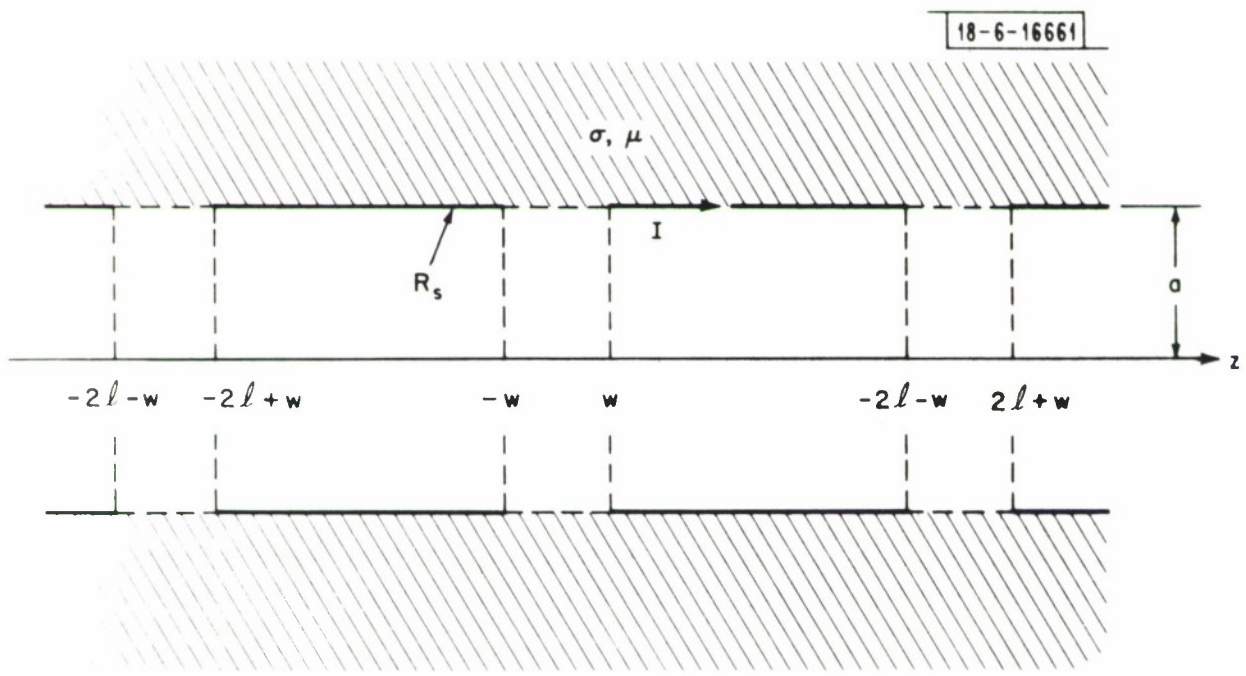


Fig. 1. Idealized model of armor on a dielectric cylinder.

where $E_g(z)$ is the z -directed total electric field in the gap (defined here to be zero for z not in the gap) and $G(z,z')$ is the Green's function giving the z -directed electric field at z due to an infinite sequence of delta functions of armor current at the locations $\pm z'$, $\pm 2\ell \pm z'$, $\pm 4\ell \pm z'$, ... The equation has been written in this form to make it valid for all z , but it now involves an additional unknown, the gap field $E_g(z)$.

The integral equation (2) is not soluble by direct means, but a variational expression [5] for the solution can be obtained by multiplying both sides by $I(z)/\ell$ and integrating over the basic interval $(0,\ell)$. By denoting the integral of $I(z)/\ell$ over this interval as I_a , the average armor current, and then dividing through by I_a^2 , one obtains

$$\frac{E_i}{I_a} = \frac{R_s}{\ell} \int_0^\ell \left[\frac{I(z)}{I_a} \right]^2 dz - \frac{1}{\ell} \int_0^\ell \frac{I(z)}{I_a} G(z,z') \frac{I(z')}{I_a} dz' dz. \quad (3)$$

The product $E_g(z)I(z)$ does not appear in this result because $I(z)$ is zero in the gap and $E_g(z)$, by definition, is zero elsewhere.

The first variation of the right side of this equation, as the quotient $I(z)/I_a$ is varied, is

$$\frac{2R_s}{\ell} \int_0^\ell \delta \left\{ \frac{I(z)}{I_a} \right\} \frac{I(z)}{I_a} dz - \frac{2}{\ell} \int_0^\ell \delta \left\{ \frac{I(z)}{I_a} \right\} G(z,z') \frac{I(z')}{I_a} dz' dz,$$

since it follows from the reciprocity theorem [6] that $G(z,z')$ is symmetric. This can be rearranged as

$$\frac{2}{\ell} \int_0^\ell \delta \left\{ \frac{I(z)}{I_a} \right\} \left[\int_0^\ell G(z, z') \frac{I(z')}{I_a} dz' - R_s \frac{I(z)}{I_a} \right] dz,$$

or, from (2),

$$\frac{2}{\ell} \int_0^\ell \delta \left\{ \frac{I(z)}{I_a} \right\} \left[E_g(z) - E_i \right] dz.$$

Now the integral over the first term in the integrand vanishes if the current variation $\delta\{I(z)/I_a\}$ is constrained to be zero when z is in the gap, since $E_g(z)$ is zero everywhere else. The integral over the second term also vanishes, since E_i , being independent of z , can be brought outside the integral operation, leaving the integral

$$\frac{1}{\ell} \int_0^\ell \delta \left\{ \frac{I(z)}{I_a} \right\} dz$$

as a factor. Interchanging the operations of variation and integration, one obtains the variation of unity, which is zero.

Thus the formula for E_i/I_a given by (3) is stationary for small variations of the normalized armor current $I(z)/I_a$ about the correct value, provided both $I(z)/I_a$ and its variation are zero in the gap.

The definition of the effective armor impedance Z_a adopted here is that it is the ratio of the average longitudinal electric field at the armor radius divided by the average longitudinal armor current. But the average long-

itudinal electric field is the uniform incident field plus the average scattered field. Thus

$$\begin{aligned} Z_a I_z &= E_i + \frac{1}{\ell} \int_0^\ell E_s(z) dz, \\ &= E_i + \frac{1}{\ell} \int_0^\ell G(z, z') I(z') dz' dz, \end{aligned} \quad (4)$$

where the lower expression on the right has been obtained by substituting for $E_s(z)$ its Green's function form.

Reversing the order of integration in (4) and using the symmetry property of the Green's function, one obtains

$$Z_a I_a = E_i + \frac{1}{\ell} \int_0^\ell I(z') \left[\int_0^\ell G(z', z) dz \right] dz', \quad (5)$$

in which the inner integral is, by definition, the electric field due to a uniform unit armor current and is therefore itself uniform. Thus the inner integral can be moved outside the outer integral operation, leaving the latter in the form of the definition of I_a , the average armor current. The result of then dividing through by I_a is

$$Z_a = \frac{E_i}{I_a} + \int_0^\ell G(z, z') dz', \quad (6)$$

which, when the variational expression (3) is substituted for E_i/I_a , becomes the required variational form for Z_a . That is

$$Z_a = \frac{R_s}{\ell} \int_0^\ell \left[\frac{I(z)}{I_a} \right]^2 dz - \frac{1}{\ell} \int_0^\ell \frac{I(z)}{I_a} G(z, z') \frac{I(z')}{I_a} dz' dz + \int_0^\ell G(z, z') dz'. \quad (7)$$

The variational property of the right side of this equation is the same as that of the right side of (3), for the additional term is independent of the armor current.

For computational purposes it is more convenient to express $I(z)$ and $G(z, z')$ as the following Fourier expansions

$$I(z) = \sum_{n=0}^{\infty} u_n \cos \frac{n\pi z}{\ell}, \quad (8)$$

where

$$u_n = \frac{\epsilon_n}{\ell} \int_0^\ell I(z) \cos \frac{n\pi z}{\ell} dz, \quad (9)$$

($\epsilon_0 = 1$, $\epsilon_n = 2$ for $n > 0$), and

$$G(z, z') = \sum_{n=0}^{\infty} G_n \cos \frac{n\pi z}{\ell} \cos \frac{n\pi z'}{\ell}. \quad (10)$$

When (8) and (10) are substituted in (7) and the identification of I_a with u_o is made, the result is

$$Z_a = R_s + \frac{1}{2} \sum_{n=1}^{\infty} \frac{u_n^2}{u_o^2} \left(R_s - \frac{\ell}{2} G_n \right). \quad (11)$$

If the cable is assumed to be surrounded with an infinite space of conducting soil, the Green's function coefficients are easily evaluated. This is done in the Appendix, the result being

$$G_n = \frac{\epsilon_n \gamma_n H_o^{(2)}(\gamma_n a)}{2\pi a \sigma \omega H_o^{(2)}(\gamma_n a)}, \quad (12)$$

where $\gamma_n = \sqrt{-j\omega\sigma\mu - n^2 \pi^2 / \ell^2}$ and $H_p^{(2)}(\gamma_n a)$ is the Hankel function of the second kind of argument $\gamma_n a$ and order p .

How close discontinuities (such as soil-air interfaces, other cables etc.) can approach the cable without seriously affecting the accuracy of (12) depends upon how far from the cable the radially-decaying Fourier components of the field extend. An important feature of (11) is that it does not include G_o , so that one concludes that (12) can be used in (11) provided external discontinuities are situated outside the region in which there exist non-negligible z -varying fields. Such a region clearly has a radius commensurable with the gap spacing.

If ℓ is small compared with a soil skin depth, then $\gamma_n \approx -jn\pi/\ell$ for $n > 0$ and the G_n , given by (12), can be rewritten in the purely real form

$$G_n = - \frac{n}{\ell^2 a\sigma} \frac{K_0(n\pi a/\ell)}{K_1(n\pi a/\ell)}, \quad n = 1, 2, \dots \quad (13)$$

where $K_p(n\pi a/\ell)$ is the modified Bessel function of the second kind of order p and argument $n\pi a/\ell$. The corresponding formula for Z_a , obtained by substituting (13) into (11) is then also purely real and its stationary point is a minimum.

III. Current Distribution

To obtain good accuracy from the variational expression (11) for Z_a it is important to make a realistic choice for the armor current distribution.

There are some obvious features which can be used as a guide:

1. When the gap spacing is very large, the armor current is essentially uniform except near the gaps. For over much of the armor section, the gaps are too far away to have any effect on the current, which therefore takes there the value it would have in a continuous armor.

2. When the gap spacing is small, the armor current will be held down to a value small compared with the continuous-armor current and so does not exhibit the "flat top" distribution characteristic of large gap spacings.

3. The current distribution is symmetrical about the armor-section mid points and, by definition, zero in the gaps.

4. If the gap spacing is small compared with a soil skin-depth, the armor current and the fringing current in the soil bridging the gaps will be defined by the equations of stationary current flow and therefore be of constant phase.

A distribution fitting this collective description over the basic interval $0 \leq z \leq 2\ell$ is

$$I(z) = \begin{cases} 0, & z \leq w \text{ and } z \leq 2\ell - w \\ 1 - \frac{\cosh[(\ell - z)/\lambda]}{\cosh[(\ell - w)/\lambda]}, & w \leq z \leq 2\ell - w \end{cases} \quad (14)$$

where λ is a parameter which is varied until (11) displays the features of a stationary point. Since $I(z)$ enters (11) only in the form $(u_n/u_0)^2$, $n = 1, 2, \dots$ there is no need to approximate any particular amplitude or constant phase. Thus, for convenience, the amplitude is of the order of unity and the phase is zero. In Fig. 2, graphs of (14) are drawn for two values of λ/ℓ which were actually encountered during the preparation of the results presented in Section V.

The u_n coefficients for this current distribution can be expressed in closed form as

$$\begin{aligned} u_0 &= 1 - \frac{w}{\ell} - \frac{\lambda}{\ell} \tanh \frac{\ell-w}{\lambda} \\ u_n &= -2 \frac{\frac{1}{n\pi} \sin \frac{n\pi w}{\ell} + \frac{\lambda}{\ell} \cos \frac{n\pi w}{\ell} \tanh \frac{\ell-w}{\lambda}}{1 + (n\pi\lambda/\ell)^2}, \quad n > 0. \end{aligned} \quad (15)$$

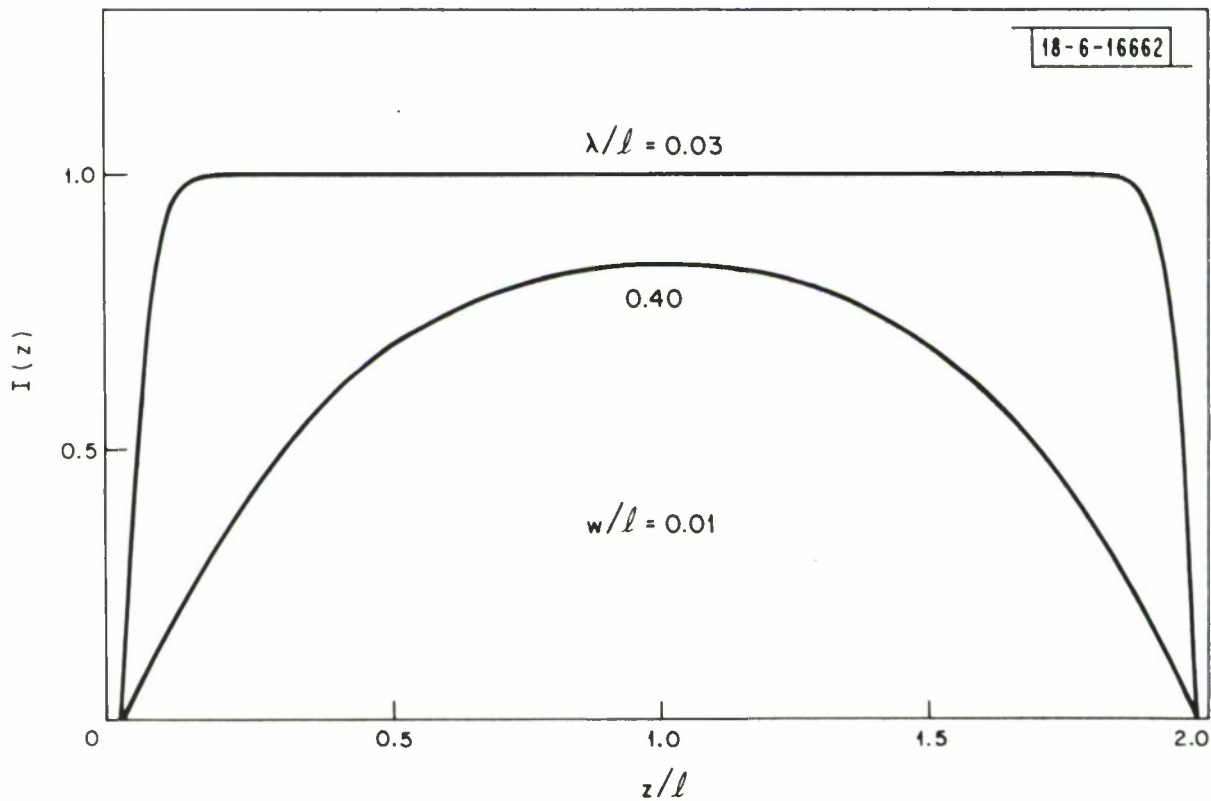


Fig. 2. The current distribution defined by (15) for two values of the normalized variational parameter λ/ℓ .

The suitability of this choice of current distribution can be checked by using a more general multi-parameter description of the distribution and then varying all the parameters in a search for the stationary value of Z_a as given by (11). If the result is close to that obtained using the single-parameter distribution (14), then one may conclude that the latter is good enough for evaluating Z_a . Such a comparison was made at four selected points in the range covered by the results presented in Section V. The outcome is described there.

IV. Application

The only assumption made about the z-directed incident field E_i has been that it is a constant over the whole surface of the dielectric. Thus the source of E_i can be an arbitrary arrangement of z-directed currents, both inside and outside the cable, provided the resulting E_i is essentially constant over the dielectric surface. Some of the currents may be the uniform impressed currents flowing in cable conductors, others may be parasitic, induced in neighboring conducting structures by the impressed currents. The essential point, however, is that in such a situation it is only the average current flowing in the armor that is of technological significance.

On the one hand, the total power dissipated per unit length is equal to the power dissipated in the driven conductors themselves plus the power emerging from the driven conductors to be dissipated in the surrounding environment. But this latter power is equal to the integral, over a unit length of the conductor surface, of the normal component of the Poynting vector. This reduces directly to the product of the uniform conductor current and the

integral (i.e., the average) of the E-field at the conductor surface. Only the average armor current need be known to evaluate its contribution to this average E-field.

On the other hand, assuming the cable is used as a buried antenna, the net current moment of the antenna is given by the integral, over the length of the antenna, of the vector sum of the cable conductor current and the armor current. If the conductor current is essentially uniform over lengths large compared with the gap spacing, again only the average armor current emerges as significant.

Evaluation of the average armor current, once Z_a is known, is carried out by regarding the armor as continuous and with its resistance per unit length replaced by Z_a . For, from (6), the condition determining the average armor current is

$$Z_a I_a = E_i + \ell G_0 I_a, \quad (16)$$

where (10) has been used to replace the integral in (6). But if the armor were continuous, I_a would be the actual uniform armor current and the condition would then be

$$I_a R_s = E_i + \int_0^{\ell} G(z, z') I_a dz'$$

which, from (10), reduces to

$$I_a R_s = E_i + \ell G_0 I_a.$$

This is identical to (16) except that Z_a has been replaced by R_s .

V. Results

Computations of Z_a were carried out using the variational form (11) into which were substituted the u_n coefficients from (15) and the G_n in zero-frequency form, given by (13). The value of Z_a corresponding to each particular set of input variables (ℓ, w, a, σ, R_s) was obtained essentially by calculating Z_a as a function of λ/ℓ , the normalized variational parameter, in sufficient detail to allow its value at the stationary (minimum) point to be determined accurately.

It was judged that interest in armor impedance at frequencies high enough for the impedance to differ markedly from the zero-frequency value would not be sufficient to warrant the presentation of a whole set of graphs like Fig. 3 covering a range of frequencies. In addition, since gapping the armor could be economically attractive only if it raises the armor impedance substantially, primary attention was given to the case $R_s = 0$, to which the three continuous curves apply. For simplicity, the results are presented in terms of the gap width g and armor-section length s instead of the "half" dimensions $w = g/2$ and $\ell = s/2$ used in the theoretical derivation.

The effect of finite armor resistance R_s on one of the curves, that corresponding to $g/a = 5.0$, is illustrated by the three broken curves. They show that if Z_a is required to exceed R_s by a factor of ten or more, then very little error is incurred by using the solid curves ($R_s = 0$) as a basis for specifying g and s .

It is of interest to note the two regimes included by the broken curves.

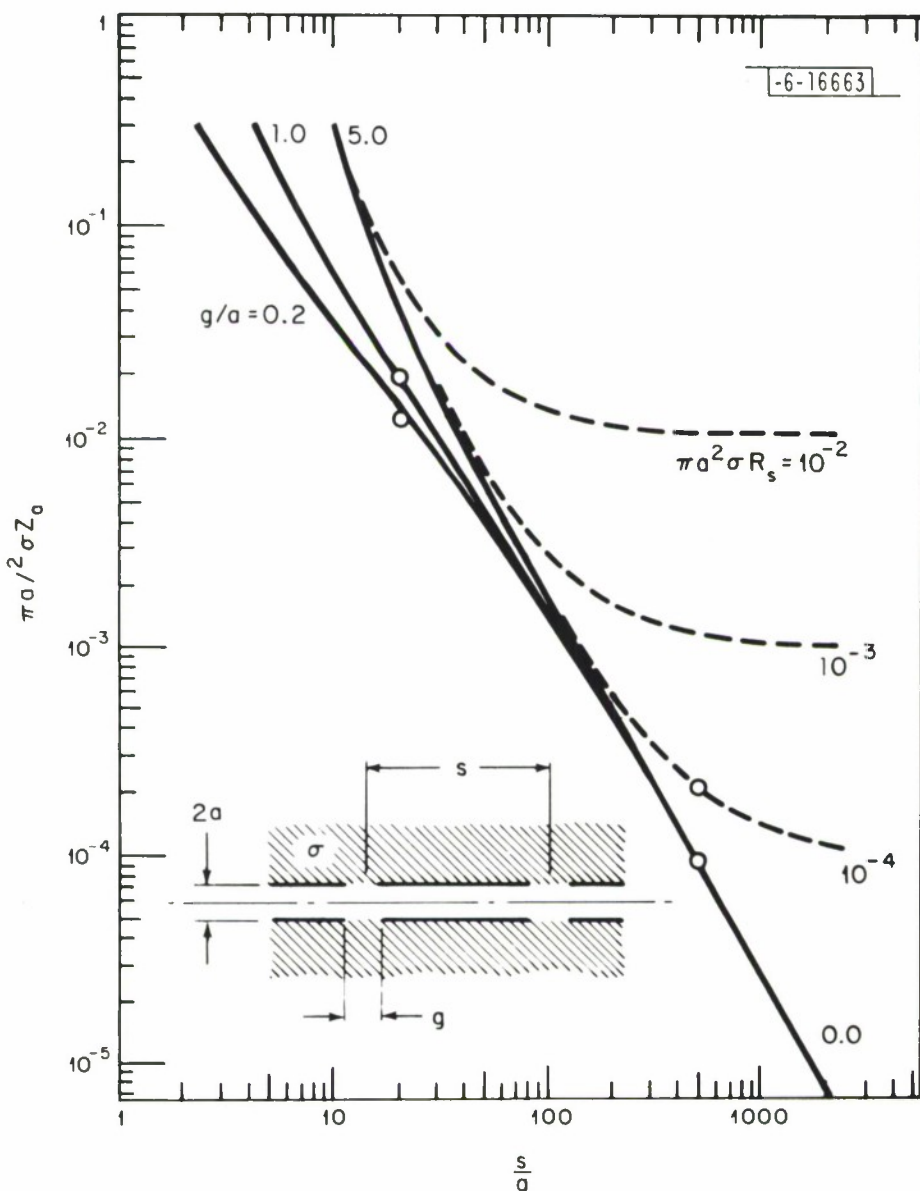


Fig. 3. The effective impedance of gapped armor at zero frequency as a function of armor-section length for selected values of gap width and armor resistance. The points are the results of the multi-parameter variational computations.

When the length of the armor sections (i.e., the gap spacing) is large, Z_a is essentially equal to R_s , but as the length is made smaller and smaller, Z_a increases until it is essentially independent of R_s but is now a function of the geometry. This is strongly reminiscent of the way the effective permeability of a ferromagnetic rod varies as a function of its length [7]. When the rod is long its effective permeability is essentially equal to the intrinsic permeability of the material, when it is short the effective permeability is geometry-limited.

A word of caution is in order concerning the interpretation of the curves for arbitrarily small gap widths. It would appear from Fig. 3 that when g is made arbitrarily small, Z_a approaches a limiting value. Theoretical considerations indicate that this is not so. The input admittance of a cylindrical dipole in free space, for example, when driven by a delta-function generator, has an infinitely large imaginary part [8]. If free space is replaced by a conducting medium, the phase angle of the admittance changes, but the infinity remains. Thus the surrounding medium short circuits completely an ideally narrow gap. One concludes therefore, that the width of the gap cannot be narrowed indefinitely without impairing its function, but in view of the weak dependence of Z_a on g/a for large g/s this may not be a constraint in practice.

As a check on the suitability of the proposed single-parameter current distribution (15), the more general distribution

$$I(z) = \begin{cases} 0, & z \leq w \text{ and } z \geq 2\ell - w \\ \sum_{m=1}^{\infty} a_m \cos \left[\frac{(2n-1)\pi}{2} \frac{\ell-z}{\ell-w} \right], & w \leq z \leq 2\ell-w \end{cases} \quad (17)$$

involving the parameters a_m was used to obtain the four points indicated in Fig. 3.

The procedure was first to take a finite Fourier transform of (17) to obtain the u_n coefficients as linear combinations of the a_m parameters and then to compute Z_a using (11) and (13). Since Z_a is independent of the absolute amplitude of $I(z)$, a_1 was set equal to unity and then the remaining a_m were varied in turn in small increments, each time retaining the value for which Z_a was a minimum. The range of m for which the a_m remained non-zero was covered repeatedly in this manner until no further change occurred in the stationary values of a_m . The final and smallest increment employed was 0.01.

Table 1 lists the set of input variables specifying each of the four points and the values of Z_a obtained using both the multi-parameter and the single-parameter descriptions of the current distribution. In the last column is the final number M of non-zero a_m parameters emerging from each multi-parameter minimum search. The multi-parameter results are also entered as points in Fig. 3.

TABLE 1
Comparison of Multi- and Single-Parameter Methods

$\frac{s}{a}$	$\frac{g}{a}$	$\pi a^2 \sigma R_s$	$\pi a^2 \sigma Z_a$		M
			Multi-Parameter	Single-Parameter	
20	0.2	0.0	1.39×10^{-2}	1.49×10^{-2}	15
20	1.0	0.0	1.89×10^{-2}	1.94×10^{-2}	9
500	5.0	0.0	9.56×10^{-5}	9.61×10^{-5}	7
500	5.0	0.0001	2.11×10^{-4}	2.10×10^{-4}	8

On the four-decade logarithmic ordinate scale used in Fig. 3, the differences between the multi-parameter results and the single-parameter results are scarcely discernible. As far as the curves presented there are concerned, therefore, one concludes that the single-parameter method is quite satisfactory.

A comparison of the entries in Table 1 on the other hand, shows that in one case the actual numerical accuracy of the single-parameter method was as bad as seven percent. This may not be acceptable in some situations, in which case the multi-parameter method should be used.

VI. Experiment

As a check on the theory, the effect of gapped armor upon the input impedance of a short length of "buried" cable was measured. A schematic diagram of the arrangement is given in Fig. 4. It shows an electrically short length of cable terminated by brass end plates and immersed in a solution of ammonium chloride in water. The end plates, being larger than a skin depth in radius, ensure that the current distribution around the cable is essentially the same as it would be were the cable of infinite length, and since

-6-16664

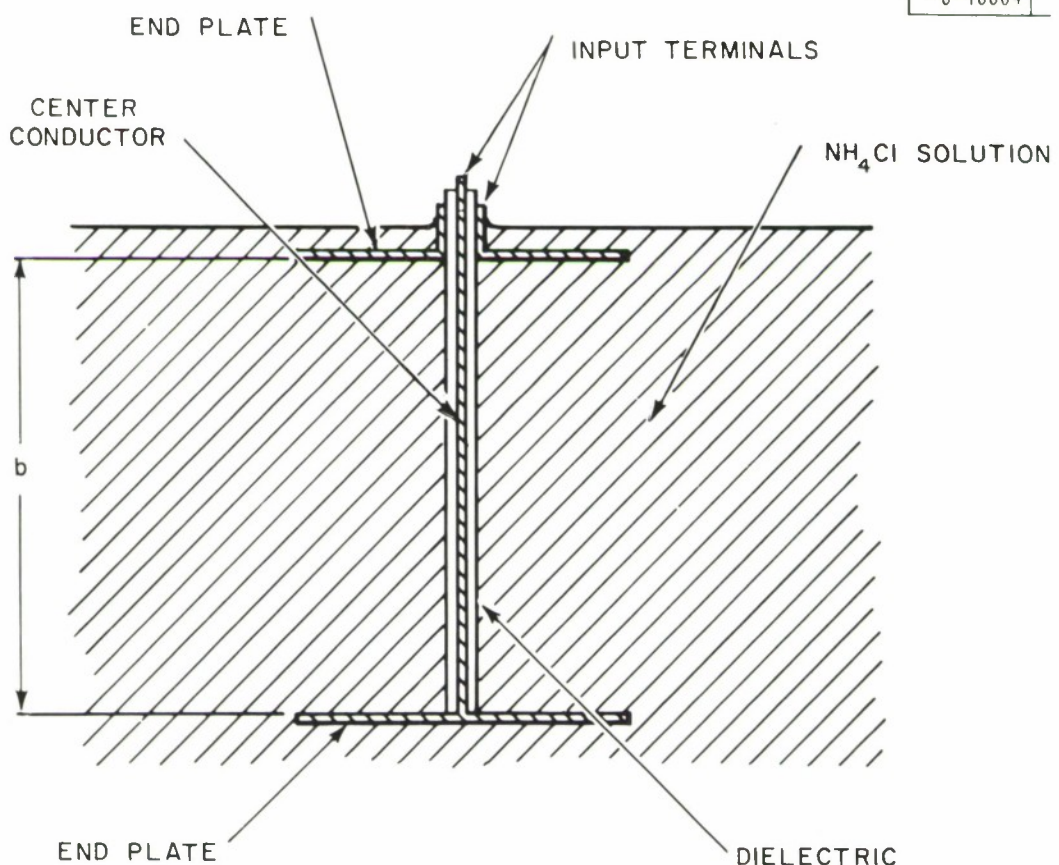


Fig. 4. Schematic diagram of experimental "cable".

the cable is electrically short, the input impedance is just the distributed series impedance per unit length multiplied by the cable length b .

Now the distributed series impedance per unit length is equal to the sum of three separate impedances. These are the internal impedance of the copper center conductor, the impedance characterizing the magnetic field energy stored in the dielectric and the external impedance. Of these, only the last is sensitive to the presence of the armor. These statements are easily verified by integrating the equation of Maxwell $\nabla \times \mathbf{E} = -j\omega\mu\mathbf{H}$ over one of the areas occupied by dielectric in Fig. 4. Since both the magnetic field in the dielectric and the electric field along the surface of the center conductor depend only on I_o , the change in input voltage due to the addition of armor is equal to (minus) the change in the integrated electric field along the outer surface of the dielectric.

From (16), the average electric field E at the armor is given by

$$E = Z_a I_a = E_i + \ell G_o I_a,$$

where E_i is here just $\ell G_o I_o$, since I_o is coaxial with and internal to I_a , and G_o given by (12) in this "infinite outer medium" situation. Eliminating I_a from these equations, one obtains

$$E = \frac{\ell G_o Z_a}{Z_a - \ell G_o} I_o.$$

In the absence of armor (that is in the limit as Z_a approaches infinity) the corresponding equation is $E = \ell G_o I_o$, so that (minus) the integrated difference divided by I_o , is the required change δZ_i in input impedance. That is

$$\delta Z_i = - \frac{(\ell G_o)^2 b}{Z_a - \ell G_o} . \quad (18)$$

The experiment consisted of applying armor, in the form of 1.3 mil adhesive copper foil, to the cable shown in Fig. 4, measuring the input impedance and then subtracting from this the input impedance measured with no armor to obtain δZ_i . A total of four different armor applications were made, all of the same gap spacing but of different gap widths. The results are shown in Table 2 and Fig. 5, together with the corresponding values of δZ_i calculated from (18) in finite-frequency form.

TABLE 2

Change in Z_i due to Armor

($f = 9.85$ MHz, $\sigma = 44$ mho/meter, $R_s = 0.0633$ ohm/meter
 $a = 1.31$ mm, $2\ell = 1$ cm, $b = 23.6$ cm)

Gap width (2w) mm	Measured δZ_i ohm	Calculated δZ_i ohm
3.5	0.25 - j 0.17	0.24 - j 0.16
2.0	0.41 - j 0.32	0.42 - j 0.29
0.5	0.87 - j 0.72	0.76 - j 0.60
0.2	0.94 - j 0.82	0.91 - j 0.74

The agreement between the calculated and the measured results is satisfactory. Since the armor was applied by hand, its placement could not be controlled to better than about 0.1 mm. This variability could account for the discrepancies between the calculated and measured results for the 0.5- and 0.2-mm gap widths.

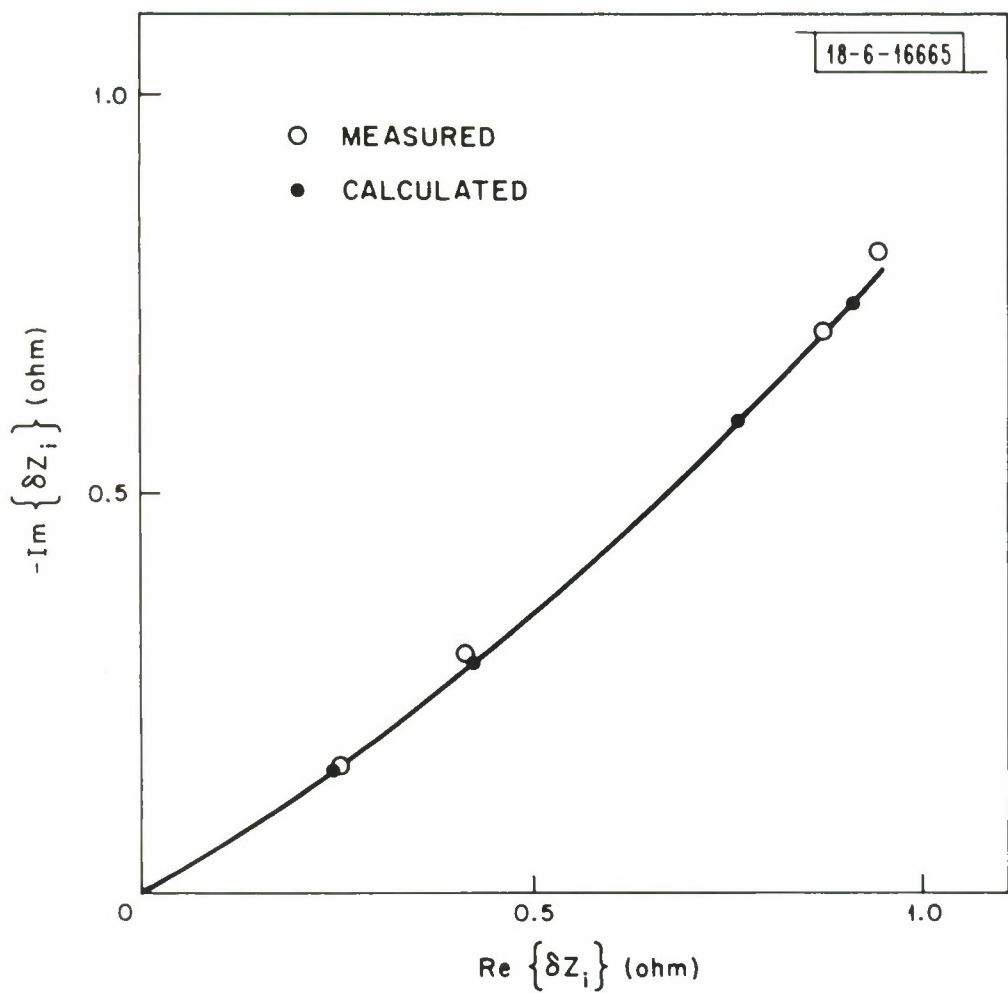


Fig. 5. Comparison between measured and calculated changes in input impedance for the experimental cable.

It should be observed that the skin-depth in copper at the frequency of measurement is not, as has been assumed, large compared with the thickness of the armor foil, but commensurable with it. Thus the armor "resistance" R_s should strictly be replaced by an impedance Z_s of comparable magnitude and non-zero phase angle. For the configuration and "soil" conductivity of the experiment, however, the effective armor impedance Z_a is completely geometry-limited ($s/a = 7.64$, $\pi a^2 \sigma R_s = 1.5 \times 10^{-5}$) and so the omission is of no consequence.

VII. Conclusions

The proposed method of calculating the effective impedance of a gapped cable armor in contact with the surrounding soil, together with the graphical results obtained from it, should be useful in situations where a continuous armor would be too conductive and some means of increasing its impedance must be found. Such a need could occur in power distribution systems and in buried antennas.

The experimental check on the method showed satisfactory corroboration for the chosen sets of geometrical and electrical quantities, but some uncertainty remains about the practical significance of the behavior of the effective armor impedance for arbitrarily small gap widths. A theoretical check of the proposed one-parameter representation for the current distribution, using a more general multi-parameter one, showed that the proposed distribution gives good accuracy.

APPENDIX

The periodicity and symmetry of the gapped-armor situation, shown in Fig. 1, allows the armor current I to be represented as

$$I = \sum_{n=0}^{\infty} u_n \cos \frac{n\pi z}{\ell} . \quad (A1)$$

Thus the delta-function current $\delta(z-z')$ is given by

$$\delta(z-z') = \frac{1}{\ell} \sum_{n=0}^{\infty} \epsilon_n \cos \frac{n\pi z}{\ell} \cos \frac{n\pi z'}{\ell} , \quad (A2)$$

where $\epsilon_0 = 1$, $\epsilon_n = 2(n > 0)$, as can be verified by multiplying both sides by $\cos(m\pi z'/\ell)$ and integrating with respect to z' from 0 to ℓ .

Now in cylindrical coordinates, the solutions of Maxwell's equations having a time behavior $\exp(j\omega t)$ and an axial behavior $\cos(n\pi z/\ell)$ are [9]:

$$E_z^{(2)}(r, z) = \alpha \gamma_n H_o^{(2)}(\gamma_n r) \cos \frac{n\pi z}{\ell} \quad (A3)$$

$$H_\phi^{(2)}(r, z) = \alpha \sigma H_1^{(2)}(\gamma_n r) \cos \frac{n\pi z}{\ell}$$

in the conducting region $r > a$, and

$$E_z^{(1)}(r, z) = \beta k_n J_o(k_n r) \cos \frac{n\pi z}{\ell} \quad (A4)$$

$$H_\phi^{(1)}(r, z) = j \beta \omega \epsilon J_1(k_n r) \cos \frac{n\pi z}{\ell}$$

in the dielectric region $r < a$. Here α and β are the unknown amplitude constants, $\gamma_n^2 = -j\omega\sigma\mu - n^2\pi^2/\ell^2$, $k_n^2 = \omega^2\epsilon\mu - n^2\pi^2/\ell^2$, σ is the conductivity of the outer region, ϵ is the permittivity in the inner region and μ is the permeability common to both regions. $H_p^{(2)}(y)$ and $J_p(y)$ are the Hankel function of the second kind and the Bessel function, respectively, each of order p and argument y . It is assumed that the exterior conducting region extends to infinity.

The boundary conditions to be satisfied at the interface are

$$E_z^{(2)}(a) - E_z^{(1)}(a) = 0 \quad (A5)$$

$$H_\phi^{(2)}(a) - H_\phi^{(1)}(a) = \cos(n\pi z/\ell)/2\pi a$$

for the current $\cos(n\pi z/\ell)$. Solving (A3), (A4) and (A5) for α , one finds

$$E_z^{(2)}(a) = \frac{k_n \gamma_n H_0^{(2)}(\gamma_n a) J_0(k_n a) \cos(n\pi z/\ell)}{2\pi a \{\sigma k_n H_1^{(2)}(\gamma_n a) J_0(k_n a) - j\omega\epsilon \gamma_n H_0^{(2)}(\gamma_n a) J_1(k_n a)\}},$$

which, for $\omega\epsilon \ll \sigma$, reduces to

$$E_z^{(2)}(a) = \frac{\gamma_n H_0^{(2)}(\gamma_n a)}{2\pi a \sigma H_1^{(2)}(\gamma_n a)} \cos \frac{n\pi z}{\ell} \quad (A6)$$

This is the electric field at the interface due to the interface current $\cos(n\pi z/\ell)$. Therefore, the total electric field due to currents superposed in the manner defined by the right side of (A2) is the required Green's func-

tion $G(z, z')$. That is

$$G(z, z') = \sum_{n=0}^{\infty} \frac{\varepsilon_n \gamma_n H_o^{(2)}(\gamma_n a)}{2\pi a \lambda \sigma H_o^{(2)}(\gamma_n a)} \cos \frac{n\pi z}{\lambda} \cos \frac{n\pi z'}{\lambda}. \quad (A7)$$

A comparison of (A7) with (10) leads to the expression for the G_n given in (12).

References

1. C. Black, "Bell Planning Tests of Anti-Gopher Gear," Electronic News 14, 54 (1969).
2. Wire and Cable Handbook (General Electric Co., Wire and Cable Dept., Bridgeport, Conn.), CM-621, p. 11.
3. Ibid., CM-650, p.4.
4. M. L. Burrows, "Armoring the Sanguine Antenna Cables," (30 January 1969), not generally available.
5. P. M. Morse and H. Feshback, Methods of Theoretical Physics (McGraw-Hill, New York, 1953), Ch. IX.
6. L. D. Landau and E. M. Lifshitz, Electrodynamics of Continuous Media (Pergamon, New York, 1960), p. 289f.
7. R. M. Bozorth, Ferromagnetism (Van Nostrand, Princeton, 1951), p. 845ff.
8. D. C. Chang, "On the Electrically Thick Cylindrical Antenna," Radio Sci. 2, 1043-1060 (1967).
9. J. A. Stratton, Electromagnetic Theory (McGraw-Hill, New York, 1941), p.524f.

OUTSIDE DISTRIBUTION LIST

Chief of Naval Operations
Attn: Capt. W. Lynch (OP941P)
The Pentagon Department of the Navy
Washington, D.C. 20350

Chief of Naval Research (Code 418)
Attn: Dr. T. P. Quinn
800 North Quincy St.
Arlington, Va. 22217

Computer Sciences Corp.
Systems Division
Attn: Mr. D. Blumberg
6565 Arlington Blvd.
Falls Church, Va. 22046
(10 copies)

Director
Defense Communications Agency
Code 960
Washington, D.C. 20305

IIT Research Institute
Attn: Mr. A. Valentino, Div. E.
10 W. 35th Street
Chicago, Illinois 60616

Naval Civil Engineering Laboratory
Attn: Mr. J. R. Allgood
Port Hueneme, CA 93043

Naval Electronics Laboratory Center
Attn: Mr. R. O. Eastman
San Diego, CA 92152

Naval Electronic Systems Command
Attn: PME-117T, Mr. J. E. DonCarlos
Dept. of the Navy
Washington, D.C. 20360
(2 copies)

Naval Electronic Systems Command
Attn: PME-117-21, Capt. J. Galloway
Department of the Navy
Washington, D.C. 20360

Mr. George Downs
Strategic Systems, Electronic Sys. Gr.
GTE Sylvania, 189 B Street
Needham, Mass. 02194

Naval Electronic Systems Command
Attn: PME-117-21A, Dr. B. Kruger
Department of the Navy
Washington, D.C. 20360

Naval Electronic Systems Command
Attn: PME-117-22, Cmdr. R. L. Gates
Department of the Navy
Washington, D.C. 20360

Naval Electronic Systems Command
Attn: PME-117-23, Mr. E. Weinberger
Department of the Navy
Washington, D.C. 20360

Naval Electronic Systems Command
Attn: PME-117-24,
Leroy S. Woznak
Department of the Navy
Washington, D. C. 20360

Naval Facilities Engineering Command
Attn: Mr. G. Hall (Code 054B)
Washington, D.C. 20390

Naval Research Laboratory A
Attn: Mr. Garner
4555 Overlook Ave. S.W.
Washington, D.C. 20390

Naval Research Laboratory
Attn: Mr. R. LaFonde
4555 Overlook Ave. S.W.
Washington, D.C. 20390

New London Laboratory
Naval Underwater Systems Center
Attn: Mr. J. Merrill
New London, CT 06320
(4 copies)

The Defense Documentation Center
Attn: DDC-TCA
Cameron Station, Building 5
Alexandria, VA 22314

Naval Research Lab
Attn: Russel M. Brown, Code 5252
4555 Overlook Ave. S.W.
Washington, D. C. 20390

UNCLASSIFIED

SECURITY CLASSIFICATION OF THIS PAGE (When Data Entered)